ORIGINAL RESEARCH

Impairments in the Default Mode and Executive Networks in Methamphetamine Users During Short-Term Abstinence

Mingqiang Gong [1,2,]*, Yunxia Shen[2,]*, Wenbin Liang[2], Zhen Zhang[3], Chunxue He[4], Mingwu Lou[2], ZiYu Xu[2]

[1]Department of Acupuncture and Moxibustion, The Fourth Clinical Medical College of Guangzhou University of Chinese Medicine, Shenzhen, People's Republic of China; [2]Department of Radiology, Longgang Central Hospital, Shenzhen, People's Republic of China; [3]Department of Radiology, The Third People's Hospital of Longgang District, Shenzhen, People's Republic of China; [4]Department of Radiology, Shenzhen Clinical Medicine College, Guangzhou University of Chinese Medicine, Shenzhen, People's Republic of China

*These authors contributed equally to this work

Correspondence: Mingwu Lou; ZiYu Xu, Department of Radiology, Longgang Central Hospital, No. 6082, Longgang Avenue, Longgang District, Shenzhen, 518000, People's Republic of China, Tel +86 13808854650; +86 13824321925, Email mingwulou@sina.com; xuziyu82@163.com

Purpose: Methamphetamine use may cause severe neurotoxicity and cognitive impairment, leading to addiction, overdose, and high rates of relapse. However, few studies have systematically focused on functional impairments detected by neuroimaging in methamphetamine abstainers (MAs) during short-term abstinence. This study aimed to investigate effective connectivity, resting-state networks, and internetwork functional connectivity in MA brains to improve clinical treatment.

Methods: Twenty MAs and 27 age- and education-matched healthy controls underwent resting-state functional magnetic resonance imaging. The amplitude of low-frequency fluctuations and Granger causality were analyzed to investigate disrupted brain regions and effective connectivity, respectively. Independent component analysis and functional network connectivity were used to identify resting-state networks and internetwork functional connectivity, respectively.

Results: Compared with healthy controls, MAs demonstrated abnormal amplitudes of low-frequency fluctuations in the bilateral precuneus, left posterior cingulate cortex (PCC), left middle frontal gyrus (MFG), left superior parietal lobule, left supplementary motor area (SMA), and left inferior parietal lobule (IPL). Moreover, MAs showed decreased effective connectivity from the left PCC to the left precuneus, increased effective connectivity from the left precuneus to the left MFG and from the right precuneus to the left SMA, and altered functional connectivity within the default mode network (DMN), frontoparietal network, sensorimotor network, ventral attention network, cerebellar network, and visual network. Importantly, hyperconnectivity between the DMN and ventral attention network and hypoconnectivity between the DMN and cerebellar network as well as the DMN and frontoparietal network were demonstrated in MAs.

Conclusion: Our study implies that in short-term methamphetamine abstinence, disruptions to the DMN and executive network may a play key role, providing new insights for early rehabilitation.

Keywords: methamphetamine, abstinence, network, Granger causality analysis, independent component analysis

Introduction

Chronic methamphetamine exposure may lead to neurotoxicity and cognitive impairments[1] in behavioral control[2] and decision making,[3] which have been closely associated with psychosis[4,5] as well as aggravated aggression and criminality,[6] and have become a concerning public health issue worldwide. It has been estimated that the total deaths due to methamphetamine overdose have increased by 90% from 2013 to 2017 in the United States.[7] In addition, approximately 61% of methamphetamine users relapse within one year and 87% relapse within five years;[8] there are no effective medications to address this issue.[9] Therefore, an exploration of the neural underpinnings of methamphetamine addiction is warranted.

Functional connectivity (FC) has been widely used to evaluate impairments in addiction.[3,10] However, FC cannot indicate the direction of interactions. Granger causality analysis (GCA) is a useful method to study effective connectivity (EC), which indicates the directionality of neural activity[11,12] and may contribute to understanding intrinsic neural mechanisms. This method has been widely used to study a variety of neurological or psychiatric disorders, such as heroin addiction[11] and cocaine addiction.[13] Recently, a study found that acute kick-boxing exercise altered EC from the prefrontal cortices to the motor cortices in methamphetamine dependencies,[14] and methamphetamine users show damaged EC in motivation circuitry.[15] However, to our knowledge, few studies have explored resting-state EC in individuals who previously used methamphetamine but currently abstain from use (methamphetamine abstainers; MAs), especially in the early stage.

Recently, the general addiction network model has been recognized to incorporate the reward network (RN), habitual network (HN), salience network (SN), executive network (EN), and default mode network (DMN).[16,17] Independent component analysis (ICA) is a data-driven method that decomposes whole-brain BOLD signals into spatially and temporally independent components (ICs) to determine differences in intranetwork and internetwork FC.[18] These ICs could be easily selected and classified into resting-state networks such as the DMN, parietal network, visual network, or other networks.[19] However, few studies have investigated alterations in resting-state networks (RSNs) and internetwork FC in MAs with less than 6 months of abstinence. We believe that exploring RSNs and network FC could elucidate the patterns of impairment in MAs, providing valuable insight into short-term abstinence treatment and future rehabilitation.

Therefore, we aimed to systematically explore the EC of regions located in the addiction network model, alterations in RSNs, and intranetwork and internetwork FC differences in short-term MAs using GCA, ICA and functional network connectivity (FNC) analyses to provide new reliable markers for rational treatment.

Materials and Methods
Subjects
MAs were recruited from a drug rehabilitation hospital in Shen Zhen, China. Healthy controls (HCs) were enrolled from the local community and matched by age, education level, and handedness. This study followed the principles of the Declaration of Helsinki and was approved by the Ethics Committee of Longgang Central Hospital. All subjects were informed of the procedure and provided informed consent before the start of the study.

The inclusion criteria for patients with methamphetamine addiction included the following items: (a) diagnosed with a substance use disorder according to the criteria in the Diagnostic and Statistical Manual of Mental Disorders, 4th edition (DSM-IV); (b) abstinent for less than 6 months; (c) no substance-use history except for methamphetamine, nicotine, and alcohol; (d) right-handed; and (e) 18 to 45 years old. The recruitment criteria for the HCs included the following: (1) good health with no severe diseases; (2) no history of substance abuse other than nicotine and alcohol; (3) right-handed; and (4) 18 to 45 years old. The exclusion criteria for all participants were as follows: (a) a history of mental disorders; (b) severe injury by collision, such as head trauma; (c) current medical illness; or (d) claustrophobia or other contraindications for magnetic resonance imaging (MRI).

Image Acquisition
The data were collected on a 3T Siemens Prisma with a 64-channel head coil. All subjects were asked to remain stationary, wear noise-cancelling earplugs, and keep their eyes closed during scanning and were instructed to avoid thinking about anything in particular or falling asleep. First, routine T2WI and fluid-attenuated inversion recovery sequences were performed to exclude individuals with gross abnormal brain structure. Then, high-resolution structural images were obtained using a gradient echo sequence with the following parameters: repetition time (TR): 2300 ms; echo time (TE): 2.32 ms; field of view (FOV): 240×240 mm^2; matrix: 256×256; slice thickness: 0.45 mm; number of sagittal slices: 208; interslice gap: 0.45 mm; voxel size: 0.9×0.9×0.9 mm^3; flip angle: 120°; scanning time: 5 minutes 21 seconds. Resting-state functional images were collected using the gradient echo-planar imaging sequence with the following parameters: TR: 2000 ms; TE: 30.0 ms; FOV: 192×192 mm^2; matrix: 64×64; slice thickness: 4.0 mm; number of axial slices: 37; interslice gap: 0.4 mm; voxel size: 3.0×3.0×4.0 mm^3; flip angle: 80°; scanning time: 6 minutes 46 seconds.

6074

International Journal of General Medicine 2022:15

Image Preprocessing

All functional images and T1 images were first converted to NIFTI format. Then, we employed DPABI software (http://rfmri.org/dpabi) to conduct standard preprocessing procedures, including slice-timing correction, realignment, coregistration, segmentation, normalization and smoothing. The first 10 time points were removed when performing slice-timing correction. To control for head-motion artifacts, subjects were excluded if maximum head motion was greater than 0.2 according the mean framewise displacement (FD) Jenkinson value, calculated by using the Friston 24 parameter model, which was determined to be superior to the 6-parameter model.[20] Reorientation of functional images and T1 images was required to improve the accuracy of the preprocessing. All images were resampled to obtain a voxel image size of $3\times3\times3$ mm^3. A 4-mm full-width at half-maximum Gaussian kernel was employed for spatial smoothing to improve the image signal-to-noise ratio and prevent the loss of useful data. To eliminate the effects of nuisance covariates, white matter signals, cerebrospinal fluid signals, linear trends, and FD Jenkinson values of head motion were regressed out.

Amplitude of Low-Frequency Fluctuations (ALFF) Analysis

The processing of the amplitude of low-frequency fluctuations (ALFF) mainly followed a previously published procedure.[21] The data were processed by REST software (http://resting-fmri.sourceforge.net). The time series of each voxel was passed through linear detrending and bandpass filtering over a range from 0.01 Hz to 0.08 Hz. Processed time series were converted by using fast Fourier transforms, and then power spectra were computed. Extraction of a root for the power spectrum across 0.01–0.08 Hz was conducted and consequently averaged for each voxel and defined as ALFF.[21] The mean ALFF of the global voxel was divided by ALFF at each voxel to obtain the standardized ALFF. Independent-samples t tests were performed to compare the MA and HC groups by REST software. Age, education level, cigarette use, and sex were regressed out as covariates. A correction for multiple comparisons was conducted using the false discovery rate (FDR), P < 0.05.

Region of Interest (ROI) Selection for GCA

Regions with significantly abnormal ALFF values and those involved in the addiction network model,[17] including the RN, HN, SN, EN, and DMN, were defined as regions of interest (ROIs). The center point of each spherical ROI was the MNI coordinate peak in the activated region of the brain, and the spherical radius of the ROI was 6 mm.

Processing of GCA

Bivariate first-order GCA was adopted by using the REST toolkit (http://resting-fmri.sourceforge.net). GCA can estimate the causal effect from ROI X to ROI Y or vice versa. The fundamental principle of GCA is determining whether a preexisting stationary time series (X) can predict another stationary time series (Y). We used the symbolic path coefficient proposed by Chen to calculate the causal effect.[22] Differences in GCA between MAs and HCs were evaluated with an independent-samples t test (p < 0.05) in SPSS (version 25.0, SPSS Inc., Chicago, IL, USA), with age, education level, cigarette use, and sex as covariates.

Processing of ICA

GIFT software (University of New Mexico, Albuquerque, NM) was applied to extract RSNs from preprocessed functional MRI (fMRI) data without prior knowledge.[23] The minimum description length[24] was used to estimate the number of independent components (ICs). Twenty-nine components were estimated. The Infomax algorithm[25] was run, and 20 iterations of the ICASSO algorithm[26] were performed to ensure the stability of the components. Individual- and group-level principal component analyses were used to reduce the dimensionality of the functional data. The group ICA type was selected for back reconstruction. Connectivity values within ICs of each subject were converted into z scores. For each IC, one-sample t tests of all subjects corrected for multiple comparisons with FDR were significant (p=0.01). A total of 15 meaningful ICs were extracted from the 24 ICs by combining the two approaches as recommended in a previous study, namely, by comparing with other templates and visual inspection. Then, the 15 ICs were classified into the following 6 functional networks: default mode network (DMN), visual network (VN), cerebellar network (CN), sensorimotor network (SMN), ventral attention network (VAN), and frontoparietal network (FPN).

FNC Analysis

After ICA, the time courses of the selected RSNs were identified by applying the spatiotemporal double regression method. FNC analyses were performed to identify FC between the time courses in two different RSNs. The time domain was limited by using a 0.00–0.25-Hz bandpass filter to cut down the disturbance from low-frequency drift and high-frequency physiological noise. FNC was calculated by employing Pearson correlation coefficients for the time courses of selected RSNs after assessing the correlation. A general linear model was constructed to determine the difference in FNC between each pair of RSNs, regressing out age, sex, education level, and abstinence duration. Corrections for multiple comparisons with FDR were performed, and the significance threshold was set at $P < 0.05$.

Results

Participant Demographics

In the total sample of 60 participants, 13 were excluded because of excessive head movement, macroscopic structural brain damage, and a history of multidrug use; 47 participants were included in the final analysis (20 in the MA group and 27 in the HC group) (Supplementary Figure 1). There was no difference in age (p = 0.639), education level (p = 0.377), or cigarette use (p = 0.334) between the MA group and HC group. The proportion of females was greater in the MA group (p = 0.043) (Table 1).

Abnormal ALFF in the Whole Brain

Compared with the HCs, the MAs showed increased ALFF in the right precuneus, left superior parietal lobule (SPL), left supplementary motor area (SMA), left superior frontal gyrus (SFG), and left inferior parietal lobule (IPL) and decreased ALFF in the left posterior cingulate cortex (PCC), left precuneus, left middle frontal gyrus (MFG), left cerebellum crus2, left fusiform, and bilateral inferior temporal gyrus (Figure 1 and Table 2).

Table 1 Demographic and Substance Use Characteristics of MAs and HCs

Characteristics	MA (n=20)	HA (n=27)	P value
Demographic Variables			
Age (y)	31.9 (6.4)	30.9 (7.7)	0.639
Sex (female/male)	5/20	1/27	0.043*
Education (y)	9.5 (2.4)	10.0 (2.1)	0.377
Methamphetamine Use Variables			
Duration (y)	7.3 (6.5)	NA	NA
Range (y)	1–20	NA	NA
Methamphetamine dose			
Amount (g/day)	0.179 (0.234)	NA	NA
Total amount (g)	800 (1689.5)	NA	NA
Range (g)	2.2–7300.0	NA	NA
Abstinence (day)	60 (40)	NA	NA
Tobacco Use Variables			
Smoker number	20	27	NA
Amount (number/day)	11.2 (6.9)	13.2 (7.4)	0.334

Note: *p < 0.05.
Abbreviations: MA, methamphetamine abstainer; HC, healthy control; y, years; SD, standard deviation.
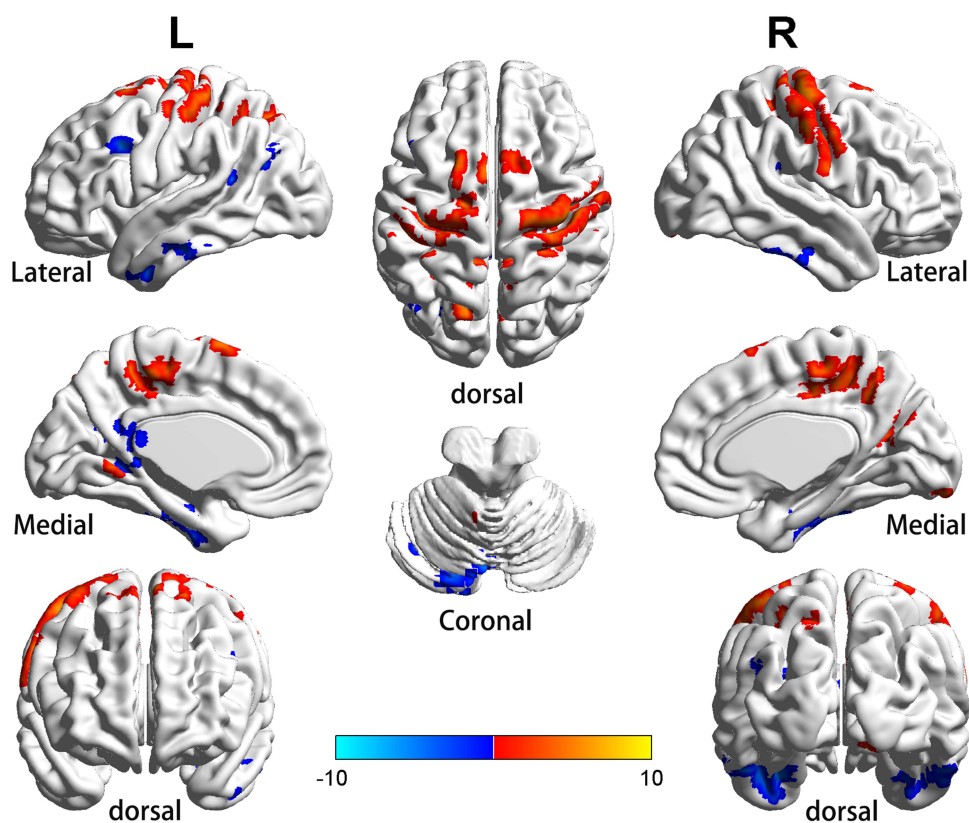
Figure 1 A significant difference in ALFF regions between the MA group and the HC group. Significant P-value with FDR correction (P < 0.05). The red zone means regions with increased ALFF, and the blue zone means regions with decreased ALFF.
Abbreviations: L, left; R, right; MA, methamphetamine abstainer; HC, healthy control; ALFF, the amplitude of low-frequency fluctuations; FDR, false discovery rate.

EC Between ROIs Involved in the Addiction Network Model

From ROI X to ROI Y, compared to the HCs, the MAs showed decreased EC from the left PCC to the left precuneus (p = 0.03) (Figure 2A) as well as from the left IPL to the left MFG (p = 0.022) (Figure 2B) and increased EC from the left precuneus to the left MFG (p = 0.021) (Figure 2C). Moreover, from ROI Y to ROI X, compared to the HCs, MAs displayed decreased EC from the right precuneus to the left PCC (p = 0.029) (Figure 2D) and increased EC from the right precuneus to the left SMA (p = 0.002) (Figure 2E), from the left MFG to the left PCC (p = 0.024) (Figure 2F) and the left SMA (p = 0.007) (Figure 2G), and from the left precuneus to the left PCC (p = 0.026) (Figure 2H). Diagram illustrated an intuitive display of the results of EC between brain regions (Figure 3).

Resting-State Networks

Using the ICA approach, we extracted 24 ICs in total, among which 15 components were classified into different meaningful RSNs. These six networks were as follows: the DMN (IC3 + IC11 + IC18) typically consisted of the bilateral precuneus, bilateral PCC, bilateral medial SFG and bilateral angular gyrus. The FPN (IC14 + IC16 + IC19) mainly included the bilateral MFG, bilateral IPL, bilateral medial SFG, bilateral left SPL, and bilateral angular gyrus. The SMN (IC7 + IC8) primarily included on the bilateral SMA, bilateral precentral gyrus, bilateral postcentral gyrus, and bilateral paracentral lobule. The VAN (IC10) mainly consisted of the bilateral supramarginal gyrus and bilateral middle cingulate cortex. The CN (IC4 + IC13 + IC24) mainly included the anterior and posterior lobes of the cerebellum. The VN (IC1 + IC5 + IC22) typically consisted of the bilateral calcarine, bilateral lingual gyrus, and bilateral occipital cortex, which included the inferior, middle, and superior occipital cortices (Figure 4).

Table 2 Regions with Significant Dysfunction Based on ALFF Between MAs and HCs

Regions	Voxels	X	Y	Z	Peak z-Value
Posterior cingulate gyrus L	25	−7	−42	16	−5.453
Superior parietal lobule L	21	−15	−72	51	5.780
Inferior parietal lobule L	24	−30	−50	45	4.071
Supplementary motor area L	28	−3	6	69	5.526
Precuneus R	42	10	−43	58	5.037
Precuneus L	28	−19	−45	3	−5.006
Superior frontal gyrus L	24	−21	12	66	4.693
Middle frontal gyrus L	23	−42	15	37	−5.720
Precentral gyrus R	114	30	−21	69	7.255
Precentral gyrus L	51	−23	−21	68	4.620
Cerebellum Crus2 L	26	−33	−70	−39	−4.261
Inferior temporal gyrus R	30	56	−33	−26	−4.804
Inferior temporal gyrus L	90	−42	−3	−36	−6.313
Fusiform L	41	−33	−12	−31	−5.588
Calcarine R	26	18	−58	17	5.535
Postcentral gyrus R	72	57	−21	46	6.554
Postcentral gyrus L	53	−37	−22	45	5.090
Middle cingulate gyrus R	30	11	−20	39	5.128
Middle cingulate gyrus L	35	−3	−39	54	6.324
Paracentral lobule R	25	6	−31	58	4.513
Paracentral lobule L	43	−4	−24	58	4.835

Note: X, Y and Z coordinates are Montreal Neurological Institute (MNI) coordinates.

Group Differences in Internetwork FNC

Compared with the HCs, the MAs showed significantly decreased FNC between the CN regions (IC24) and DMN regions (IC3) as well as between the DMN regions (IC11) and FPN regions (IC16). In addition, compared with the HCs, the MAs exhibited significantly increased FNC between the DMN regions (IC3) and the VAN (IC10) (Figure 5).

Discussion

This study revealed systematic functional impairments in short-term MAs by performing ALFF, GCA, ICA, and FNC. Specifically, compared with the HCs, the MAs demonstrated altered ALFF and EC in various regions, including the bilateral precuneus, left PCC, left MFG, left SMA, and left IPL. Importantly, we observed impaired brain networks, including the DMN, FPN, SN, VAN, CN, and VN, and significantly damaged internetwork FC between the DMN-CN, DMN-FPN, and DMN-VAN.

Alterations in the Default Mode Network

The DMN, also called the self-directed network, is responsible for self-awareness, emotion, and rumination.[19] Accumulating evidence has shown that both the PCC and the precuneus are components of a midline core network within the DMN associated with self-related decision-making.[27] The PCC supports internally directed cognition and regulates attention and conscious awareness,[28] whereas the precuneus contributes to self-monitoring and exteroceptive processes related to responses to conditioned cues.[29] Previous studies have shown weaker activation in the precuneus[30] and smaller cortical volume and thinner cortex in the PCC[31] of MAs. In our study, short-term MAs showed decreased ALFF in the left PCC, and the left precuneus in this region was hypoactive. Moreover, the left PCC had a negative influence on the left precuneus, and the left precuneus had a positive effect on the left PCC, which may imply a disrupted state of information transfer within the DMN.
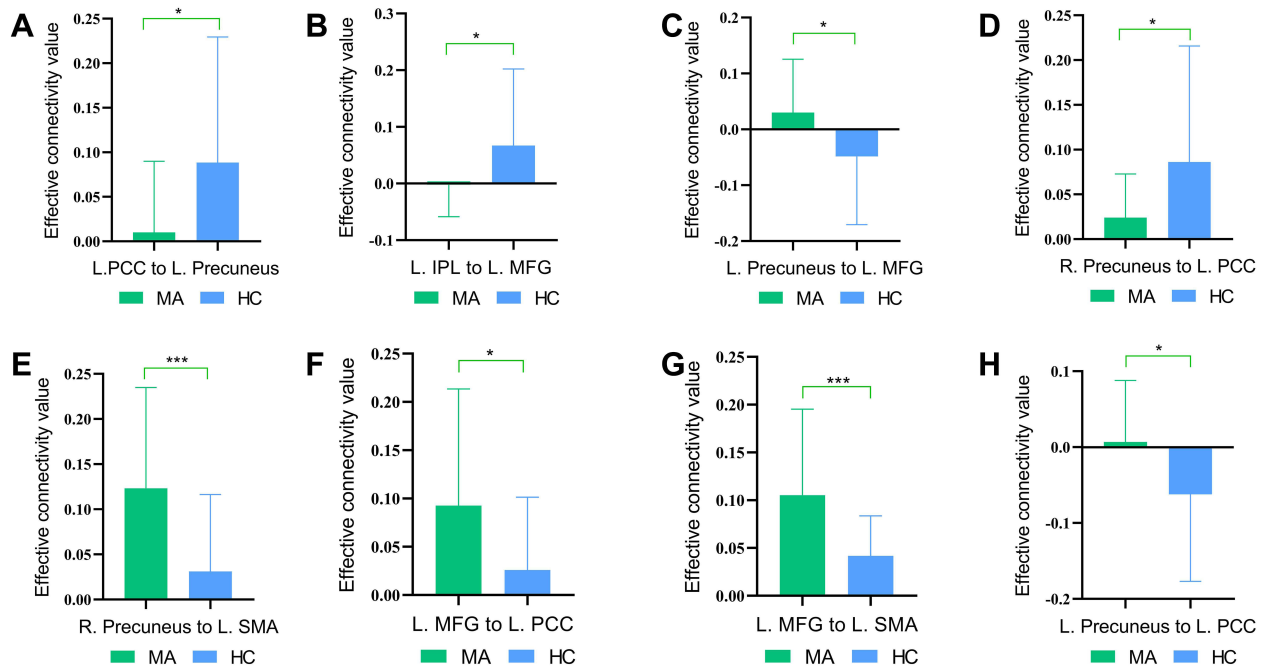
Figure 2 A significant difference in effective connectivity between the MA group and the HC group. (**A**) Decreased EC from the left PCC to the left precuneus. (**B**) Decreased EC from the left IPL to the left MFG. (**C**) Increased EC from the left precuneus to the left MFG. (**D**) Decreased EC from the right precuneus to the left PCC. (**E**) Increased EC from the right precuneus to the left SMA. (**F**) Increased EC from the left MFG to the left PCC. (**G**) Increased EC from the left MFG to the left SMA. (**H**) Increased EC from the left precuneus to the left PCC.

Note: *$p < 0.05$; ***$p < 0.005$.

Abbreviations: EC, effective connectivity; PCC, posterior cingulate cortex; MFG, middle frontal gyrus; IPL, inferior parietal lobule; SMA, supplementary motor area; MA, methamphetamine abstainer; HC, healthy control; L, left; R, right.
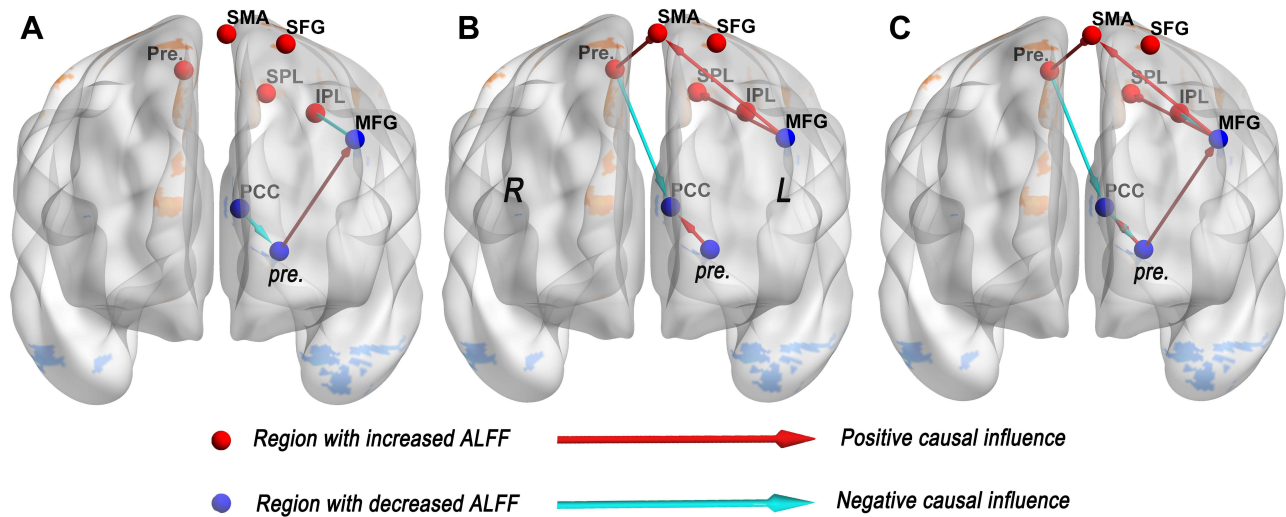
Figure 3 Alteration Effective connectivity between two groups. (**A**) Effective connectivity from ROI X to ROI Y. (**B**) Effective connectivity from ROI Y to ROI X. (**C**) Effective connectivity of the whole brain. Red nodes indicate regions with increased ALFF, and blue nodes suggest regions with decreased ALFF. Red arrows represent hyper-effective connectivity, and green arrows represent hypo-effective connectivity.

Abbreviations: SMA, supplementary motor area; SFG, superior frontal gyrus; SPL, superior parietal lobule; IPL, inferior parietal lobule; MFG, middle frontal gyrus; PCC, posterior cingulate cortex; Pre, precuneus; L, left; R, right.

More importantly, although altered FC correlates with DMN activation in MAs after six months of abstinence,[32] our study confirmed DMN function is impaired in MAs with less than six months of abstinence. Taken together, the alterations in the DMN in short-term MAs may imply disrupted self-awareness and self-related decision-making.
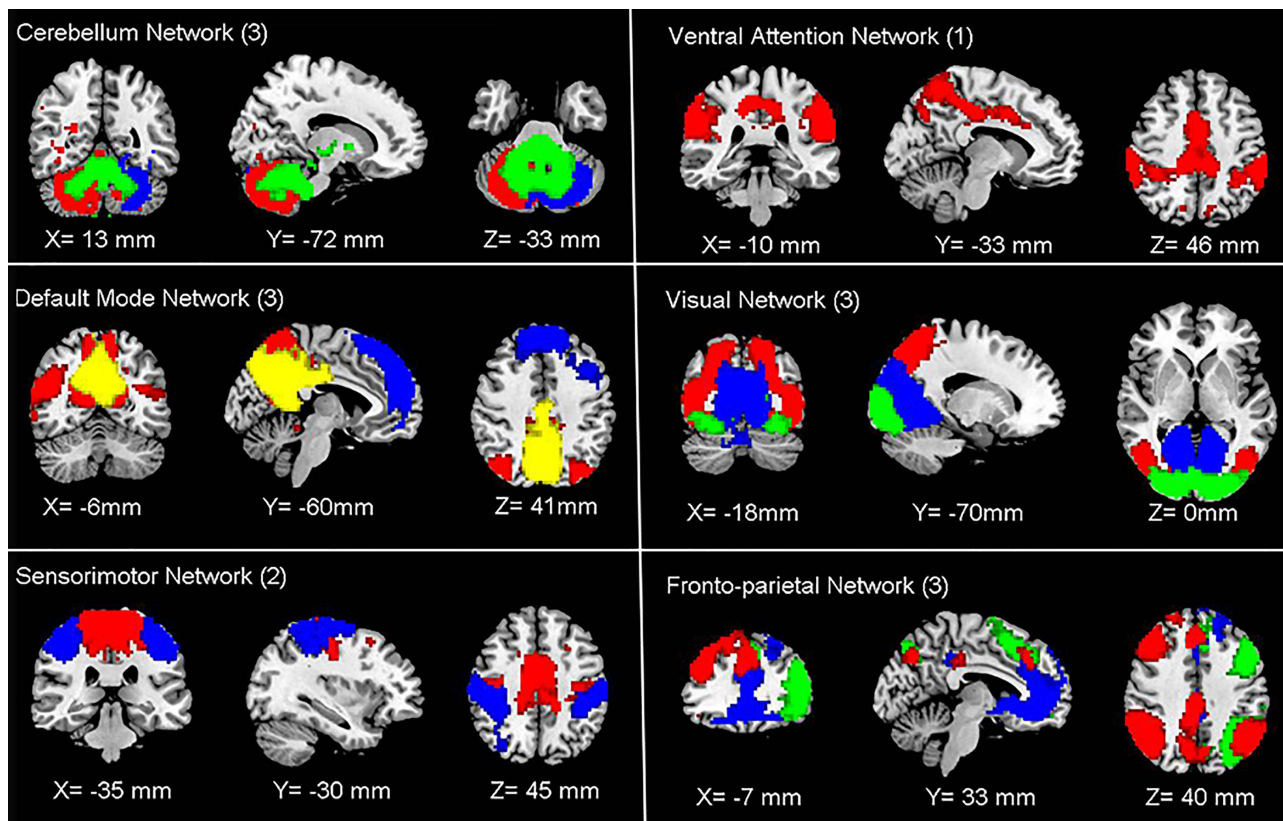
Figure 4 Functional associated resting-state networks (RSNs). The spatial maps of 15 independent components were identified and classified as RSNs for function network connectivity analysis.
Abbreviations: CN, cerebellum network; DMN, default mode network; SMN, sensorimotor network; VAN, ventral attention network; VN, visual network; FPN, frontoparietal network.

Alterations in the Executive Network

The EN is one of the important networks associated with addiction and is considered to enable goal-directed behavior.[17] The SPL, a part of the EN, plays an essential role in the integration process[33] and engages working memory[34] as well as visuospatial and somatosensory integration to achieve executive function.[35] Increased ALFF in the SPL, as found in our study, may imply cognitive impairment.[36] In addition, the SPL is involved in the FPN, also known as the central executive network.[37,38] The MFG and SMA are involved in frontoparietal connectivity related to the performance of new actions, inhibition of behavior,[39] sensation seeking, and impulsivity.[40] Greater activation in the SMA in MAs is associated with drug-related stimuli.[41] In the current study, increased ALFF in the SMA may imply that impulse control is not restored in short-term MAs. No study has observed toxic effects of drugs in the FPN except cocaine.[42] In our study, the damaged resting-state FPN in short-term MAs may be a new finding. Moreover, we also observed positive EC from the left MFG to the left SPL/SMA within the FPN. Overall, abnormal function of the FPN (EN) may be related to impairments in inhibition and information integration; it may thus represent a potential therapeutic target.

Interaction of Resting-State Networks

Increasing evidence suggests that interactions between different networks underlie the neural mechanisms of normal function. Previous studies have found that substance abuse of drugs other than methamphetamine disrupt the DMN and the executive control network.[27] Our results confirm the decreased DMN-CN connectivity. The cerebellum has extensive associations with substance addiction, including the use of cocaine, opioids, nicotine and alcohol,[43] based on its monosynaptic projections to the ventral tegmental area (VTA).[44] Furthermore, the VTA targets the prefrontal cortex, which is involved in the DMN,[44] supporting the idea of connections between the DMN and CN. After six months of abstinence, MAs exhibited disrupted FC between the
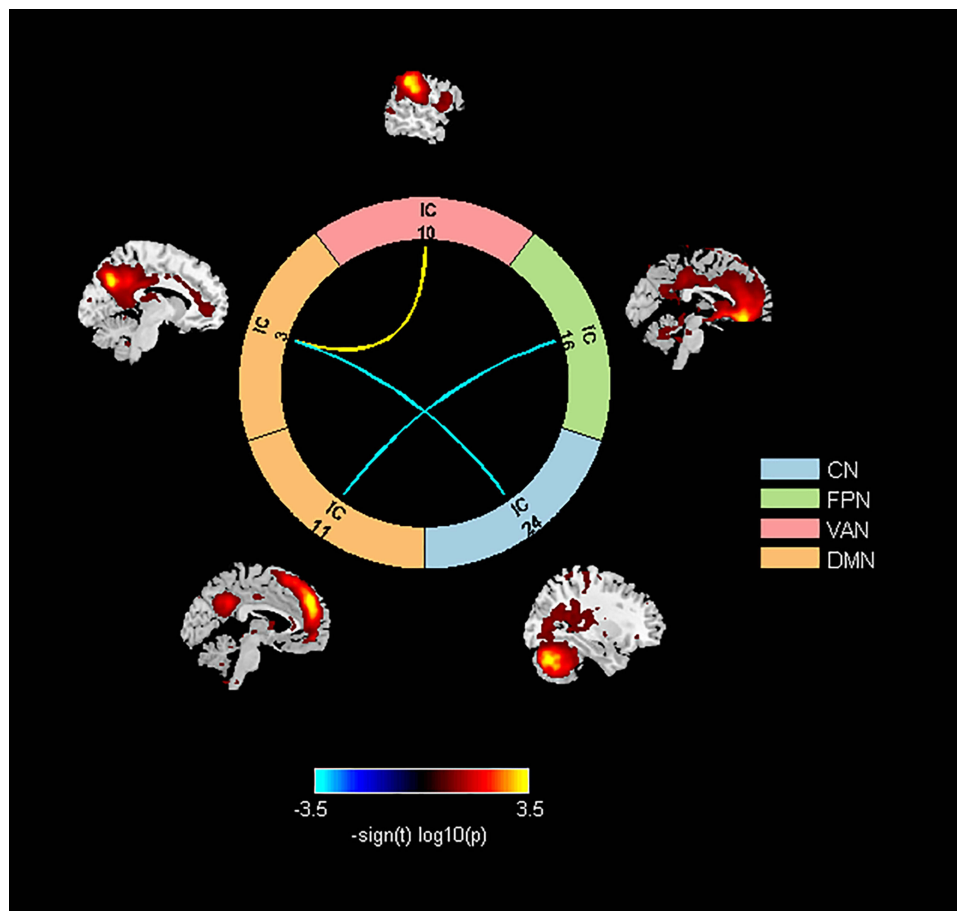
Figure 5 Group significant differences of inter-network connectivity.
Abbreviations: DMN, default mode network; VAN, ventral attention network; FPN, frontoparietal network; CN, cerebellum network; IC, independent component.

cerebellum and DMN.[32] Our findings further demonstrated decreased DMN-CN FC in short-term MAs, implying that impaired DMN-CN connectivity is characteristic of marked damage.

The FPN is considered crucial to cognitive control.[38] Coordination between the DMN and FPN is associated with internal thought.[45] The chronic effects of betel nuts, a kind of psychoactive substance, damage the DMN and FPN and contribute to compulsive substance use.[46] Similarly, individuals with internet gaming disorder also show significantly decreased involvement of the DMN and FPN.[47] Decreased DMN-FPN connectivity, as found in our study, may imply impairment of internal thoughts and cognitive control. The DMN is also responsible for introspection, and the VAN facilitates to attention to prominent features of the external environment.[48] Importantly, a meta-analysis revealed that individuals with substance use disorder, compared with healthy subjects, showed hypoactivity in regions involved in the DMN and VAN.[49] In the current study, increased connectivity between the DMN and VAN may influence integration between the external environment and introspection.

This study has some limitations. First, this was a cross-sectional study using a series of methods to evaluate cerebral injury in MAs with less than six months of abstinence; data were collected in the resting state, which does not provide information on dynamic changes. Second, our results are not consistent with structural MRI damage and failed to link functional and structural impairments. Third, the number of female subjects was limited, the sex ratio was biased, and the sample size was relatively small. Fourth, no urinalysis was performed for MAs, but this was unlikely to be an issue since all MAs were currently abstinent. Fifth, individuals frequently struggle to recall their own alcohol consumption; hence, collecting data on alcohol consumption is prone to substantial uncertainty. This study did not record the amount of alcohol that individuals consumed and did not explore its potential to influence the results, which may be considered a limitation. Sixth, we did not discuss abstinence duration and brain recovery in this manuscript, as we found no

statistically significant links between withdrawal time, ALFF level, and EC. This lack of association may be related to variation in withdrawal duration and the small sample size.

Conclusion

In conclusion, we observed systematic alterations in the brains of short-term MAs (less than six months of abstinence) by using methods such as ALFF, GCA, ICA, and FNC. We found that the DMN and EN (FPN) play crucial roles in short-term methamphetamine abstinence in relation to functional deficiencies in self-awareness, introspection, and executive function; these areas may serve as therapeutic targets. Our findings expand current understanding of the mechanisms disrupted in MAs and provide useful information for early detoxification and rehabilitation.

Abbreviations

MA, methamphetamine abstainer; DMN, default mode network; HC, healthy control; FPN, frontoparietal network; ALFF, low-frequency fluctuations; VAN, ventral attention network; GCA, Granger causality analysis; CN, cerebellum network; EC, effective connectivity; EN, executive network; ICA, Independent component analysis; FC, functional connectivity; FNC, functional network connectivity; ROI, region of interest; PCC, posterior cingulate cortex; IC, independent component; MFG, middle frontal gyrus; FDR, false discovery rate; IPL, inferior parietal lobule; VN, visual network; SMA, supplementary motor area; RSN, resting-state network.

Ethics Statement

The studies involving human participants were reviewed and approved by the Ethics Committee of Longgang Central Hospital. The patients/participants provided their written informed consent to participate in this study.

Acknowledgments

Author Contributions

All authors made a significant contribution to the work reported, like in the conception, study design, execution, acquisition of data, analysis, and interpretation. All took part in whitening, revising, and reviewing the article. All authors have agreed on the journal to which the article will be submitted, and will reviewed and agree on all versions of the article before submission, during revision, the final version accepted for publication, and any significant changes introduced at the proofing stage. Authors will also agree to take responsibility and be accountable for the contents of the article.

Disclosure

The authors declare that the research was conducted in the absence of any commercial or financial relationships that could be construed as a potential conflict of interest.

References

1. Van Hedger K, Keedy SK, Mayo LM, Heilig M, de Wit H. Neural responses to cues paired with methamphetamine in healthy volunteers. *Neuropsychopharmacology.* 2018;43(8):1732–1737. doi:10.1038/s41386-017-0005-5
2. Hu Y, Salmeron BJ, Krasnova IN, et al. Compulsive drug use is associated with imbalance of orbitofrontal- and prelimbic-striatal circuits in punishment-resistant individuals. *Proc Natl Acad Sci USA.* 2019;116(18):9066–9071. doi:10.1073/pnas.1819978116
3. Kohno M, Morales AM, Ghahremani DG, Hellemann G, London ED. Risky decision making, prefrontal cortex, and mesocorticolimbic functional connectivity in methamphetamine dependence. *JAMA Psychiatry.* 2014;71(7):812–820. doi:10.1001/jamapsychiatry.2014.399
4. Greening DW, Notaras M, Chen M, et al. Chronic methamphetamine interacts with BDNF Val66Met to remodel psychosis pathways in the mesocorticolimbic proteome. *Mol Psychiatry.* 2019;26(8):4431–4447. doi:10.1038/s41380-019-0617-8
5. Jones CM, Compton WM, Mustaquim D. Patterns and characteristics of methamphetamine use among adults - United States, 2015–2018. *Morb Mortal Wkly Rep.* 2020;69(12):317–323. doi:10.15585/mmwr.mm6912a1

6. Darke S, Kaye S, McKetin R, Duflou J. Major physical and psychological harms of methamphetamine use. *Drug Alcohol Rev*. 2008;27(3):253–262. doi:10.1080/09595230801923702

7. Kariisa M, Scholl L, Wilson N, Seth P, Hoots B. Drug overdose deaths involving cocaine and psychostimulants with abuse potential - United States, 2003–2017. *Morb Mortal Wkly Rep*. 2019;68(17):388–395. doi:10.15585/mmwr.mm6817a3

8. Brecht ML, Herbeck D. Time to relapse following treatment for methamphetamine use: a long-term perspective on patterns and predictors. *Drug Alcohol Depend*. 2014;139:18–25. doi:10.1016/j.drugalcdep.2014.02.702

9. Chan B, Freeman M, Kondo K, et al. Pharmacotherapy for methamphetamine/amphetamine use disorder-a systematic review and meta-analysis. *Addiction*. 2019;114(12):2122–2136. doi:10.1111/add.14755

10. Weafer J, Van Hedger K, Keedy SK, Nwaokolo N, de Wit H. Methamphetamine acutely alters frontostriatal resting state functional connectivity in healthy young adults. *Addict Biol*. 2020;25(3):e12775. doi:10.1111/adb.12775

11. Zhang Y, Li Q, Wen X, et al. Granger causality reveals a dominant role of memory circuit in chronic opioid dependence. *Addict Biol*. 2017;22 (4):1068–1080. doi:10.1111/adb.12390

12. Cottam WJ, Iwabuchi SJ, Drabek MM, Reckziegel D, Auer DP. Altered connectivity of the right anterior insula drives the pain connectome changes in chronic knee osteoarthritis. *Pain*. 2018;159(5):929–938. doi:10.1097/j.pain.0000000000001209

13. Zhang S, Zhornitsky S, Wang W, Dhingra I, Le TM, Li CR. Cue-elicited functional connectivity of the periaqueductal gray and tonic cocaine craving. *Drug Alcohol Depend*. 2020;216:108240. doi:10.1016/j.drugalcdep.2020.108240

14. Bu L, Qi L, Yan W, et al. Acute kick-boxing exercise alters effective connectivity in the brain of females with methamphetamine dependencies. *Neurosci Lett*. 2020;720:134780. doi:10.1016/j.neulet.2020.134780

15. Mansoory MS, Sharini H, Behboudi M, Farnia V, Khodamoradi M, Alikhani M. Resting-state effective connectivity in the motive circuit of methamphetamine users: a case controlled fMRI study. *Behav Brain Res*. 2020;383:112498. doi:10.1016/j.bbr.2020.112498

16. Volkow ND, Fowler JS, Wang G-J. The addicted human brain: insights from imaging studies. *J Clin Invest*. 2003;111(10):1444–1451. doi:10.1172/JCI18533

17. Zilverstand A, Huang AS, Alia-Klein N, Goldstein RZ. Neuroimaging impaired response inhibition and salience attribution in human drug addiction: a systematic review. *Neuron*. 2018;98(5):886–903. doi:10.1016/j.neuron.2018.03.048

18. Xing C, Zhang J, Cui J, et al. Disrupted functional network connectivity predicts cognitive impairment in presbycusis patients. *Front Aging Neurosci*. 2020;12:246. doi:10.3389/fnagi.2020.00246

19. Luo L, Wu H, Xu J, et al. Abnormal large-scale resting-state functional networks in drug-free major depressive disorder. *Brain Imaging Behav*. 2021;15(1):96–106. doi:10.1007/s11682-019-00236-y

20. Yan CG, Cheung B, Kelly C, et al. A comprehensive assessment of regional variation in the impact of head micromovements on functional connectomics. *Neuroimage*. 2013;76:183–201. doi:10.1016/j.neuroimage.2013.03.004

21. Zang YF, He Y, Zhu CZ, et al. Altered baseline brain activity in children with ADHD revealed by resting-state functional MRI. *Brain Dev*. 2007;29 (2):83–91. doi:10.1016/j.braindev.2006.07.002

22. Palaniyappan L, Simmonite M, White TP, Liddle EB, Liddle PF. Neural primacy of the salience processing system in schizophrenia. *Neuron*. 2013;79(4):814–828. doi:10.1016/j.neuron.2013.06.027

23. Beckmann CF, Smith SM. Probabilistic independent component analysis for functional magnetic resonance imaging. *IEEE Trans Med Imaging*. 2004;23(2):137–152. doi:10.1109/TMI.2003.822821

24. Li YO, Adali T, Calhoun VD. Estimating the number of independent components for functional magnetic resonance imaging data. *Hum Brain Mapp*. 2007;28(11):1251–1266. doi:10.1002/hbm.20359

25. Bell AJ, Sejnowski TJ. An information-maximization approach to blind separation and blind deconvolution. *Neural Comput*. 1995;7(6):1129–1159. doi:10.1162/neco.1995.7.6.1129

26. Himberg J, Hyvarinen A, Esposito F. Validating the independent components of neuroimaging time series via clustering and visualization. *Neuroimage*. 2004;22(3):1214–1222. doi:10.1016/j.neuroimage.2004.03.027

27. Zhang R, Volkow ND. Brain default-mode network dysfunction in addiction. *Neuroimage*. 2019;200:313–331. doi:10.1016/j.neuroimage.2019.06.036

28. Leech R, Sharp DJ. The role of the posterior cingulate cortex in cognition and disease. *Brain*. 2014;137(Pt 1):12–32. doi:10.1093/brain/awt162

29. DeWitt SJ, Ketcherside A, McQueeny TM, Dunlop JP, Filbey FM. The hyper-sentient addict: an exteroception model of addiction. *Am J Drug Alcohol Abuse*. 2015;41(5):374–381. doi:10.3109/00952990.2015.1049701

30. Droutman V, Xue F, Barkley-Levenson E, et al. Neurocognitive decision-making processes of casual methamphetamine users. *Neuroimage Clin*. 2019;21:101643. doi:10.1016/j.nicl.2018.101643

31. MacDuffie KE, Brown GG, McKenna BS, et al. Effects of HIV infection, methamphetamine dependence and age on cortical thickness, area and volume. *Neuroimage Clin*. 2018;20:1044–1052. doi:10.1016/j.nicl.2018.09.034

32. Li X, Su H, Zhong N, et al. Aberrant resting-state cerebellar-cerebral functional connectivity in methamphetamine-dependent individuals after six months abstinence. *Front Psychiatry*. 2020;11:191. doi:10.3389/fpsyt.2020.00191

33. Collette F, Van der Linden M, Laureys S, et al. Exploring the unity and diversity of the neural substrates of executive functioning. *Hum Brain Mapp*. 2005;25(4):409–423. doi:10.1002/hbm.20118

34. Necka E, Gruszka A, Hampshire A, et al. The effects of working memory training on brain activity. *Brain Sci*. 2021;11:2. doi:10.3390/brainsci11020155

35. Gamberini M, Passarelli L, Fattori P, Galletti C. Structural connectivity and functional properties of the macaque superior parietal lobule. *Brain Struct Funct*. 2020;225(4):1349–1367. doi:10.1007/s00429-019-01976-9

36. Zhuang L, Ni H, Wang J, et al. Aggregation of vascular risk factors modulates the amplitude of low-frequency fluctuation in mild cognitive impairment patients. *Front Aging Neurosci*. 2020;12:604246. doi:10.3389/fnagi.2020.604246

37. Lobanov OV, Quevedo AS, Hadsel MS, Kraft RA, Coghill RC. Frontoparietal mechanisms supporting attention to location and intensity of painful stimuli. *Pain*. 2013;154(9):1758–1768. doi:10.1016/j.pain.2013.05.030

38. Zanto TP, Gazzaley A. Fronto-parietal network: flexible hub of cognitive control. *Trends Cogn Sci*. 2013;17(12):602–603. doi:10.1016/j.tics.2013.10.001

39. Nachev P, Kennard C, Husain M. Functional role of the supplementary and pre-supplementary motor areas. *Nat Rev Neurosci*. 2008;9(11):856–869. doi:10.1038/nrn2478

40. Holmes AJ, Hollinshead MO, Roffman JL, Smoller JW, Buckner RL. Individual differences in cognitive control circuit anatomy link sensation seeking, impulsivity, and substance use. *J Neurosci*. 2016;36(14):4038–4049. doi:10.1523/JNEUROSCI.3206-15.2016

41. Chen S, Huang S, Yang C, et al. Neurofunctional differences related to methamphetamine and sexual cues in men with shorter and longer term abstinence methamphetamine dependence. *Int J Neuropsychopharmacol*. 2020;23(3):135–145. doi:10.1093/ijnp/pyz069

42. Barros-Loscertales A, Costumero V, Rosell-Negre P, Fuentes-Claramonte P, Llopis-Llacer JJ, Bustamante JC. Motivational factors modulate left frontoparietal network during cognitive control in cocaine addiction. *Addict Biol*. 2020;25(4):e12820. doi:10.1111/adb.12820

43. Moulton EA, Elman I, Becerra LR, Goldstein RZ, Borsook D. The cerebellum and addiction: insights gained from neuroimaging research. *Addict Biol*. 2014;19(3):317–331. doi:10.1111/adb.12101

44. Carta I, Chen CH, Schott AL, Dorizan S, Khodakhah K. Cerebellar modulation of the reward circuitry and social behavior. *Science*. 2019;363:6424. doi:10.1126/science.aav0581

45. Smallwood J, Brown K, Baird B, Schooler JW. Cooperation between the default mode network and the frontal-parietal network in the production of an internal train of thought. *Brain Res*. 2012;1428:60–70. doi:10.1016/j.brainres.2011.03.072

46. Linli Z, Huang X, Liu Z, Guo S, Sariah A. A multivariate pattern analysis of resting-state functional MRI data in naive and chronic betel quid chewers. *Brain Imaging Behav*. 2021;15(3):1222–1234. doi:10.1007/s11682-020-00322-6

47. Zhou WR, Wang M, Zheng H, Wang MJ, Dong GH. Altered modular segregation of brain networks during the cue-craving task contributes to the disrupted executive functions in internet gaming disorder. *Prog Neuropsychopharmacol Biol Psychiatry*. 2021;107:110256. doi:10.1016/j.pnpbp.2021.110256

48. Palanca BJA, Avidan MS, Mashour GA. Human neural correlates of sevoflurane-induced unconsciousness. *Br J Anaesth*. 2017;119(4):573–582. doi:10.1093/bja/aex244

49. Qiu Z, Wang J. Altered neural activities during response inhibition in adults with addiction: a voxel-wise meta-analysis. *Psychol Med*. 2021;51(3):387–399. doi:10.1017/S0033291721000362